Complex Formation between Polyelectrolyte and Oppositely Charged Mixed Micelles: Soluble Complexes vs Coacervation

Yingjie Li and Paul L. Dubin*

Department of Chemistry, Indiana University-Purdue University, Indianapolis, Indiana 46202

Henry A. Havel and Shun L. Edwards

Biopharmaceutical Development, Eli Lilly and Co., Indianapolis, Indiana 46285

Herbert Dautzenberg

Max Planck Institute for Colloid and Interface Research, Teltow-Seehof O-1530, Germany

Received January 11, 1995. In Final Form: April 24, 1995®

The system comprised of poly(dimethyldiallylammonium chloride) (PDMDAAC) and oppositely charged mixed micelles of Triton X-100 (TX100) and sodium dodecylsulfate (SDS) displays several states, including coacervate and various soluble complexes. The phase boundary for the equilibrium between soluble complexes and coacervate ("associative phase separation" according to Piculell and Lindman) for 0.4 M NaCl and Y = [SDS]/([SDS] + [TX100]) = 0.3 was constructed. Coacervation takes place when the total concentration of surfactants and PDMDAAC is very low and the weight ratio of PDMDAAC to TX100-SDS, *W*, is close to 0.09, a stoichiometry which corresponds to a 1:1 charge ratio of PDMDAAC to TX100-SDS. The phase separation region region is over 2 orders of magnitude smaller than that of most polyelectrolyte/oppositely charged surfactant systems (without nonionic surfactant). In the soluble complex region, dilution with 0.4 M NaCl is seen to disaggregate multipolymer complexes into intrapolymer complexes, but the electrophoretic mobility of the complexes remains unchanged. The electrophoretic mobility of complexes changes from negative to positive with increasing *W* and approaches zero at incipient coacervation. In the soluble complex region, an increase in *W* leads to an increase in the concentration of intrapolymer complexes, followed by formation of interpolymer complexes and coacervation. Further increase in *W* redissolves the coacervate. The formation of soluble complexes over a wide range of conditions supports the theoretical models of complex coacervation by Veis and by Tainaka. However, the interpolymer complex formation that is observed in this system is not considered in either theory.

Introduction

Complex formation between polyelectrolytes and oppositely charged surfactants has been a subject of intense research effort (for reviews, see refs 1–6). However, most of the published studies on the polyelectrolyte/surfactant complexes have involved surfactants at such low concentrations that micelles are absent. The interaction between polyelectrolytes and oppositely charged surfactants is dominated by strong electrostatic forces which cause the association to start at a very low surfactant concentration, known as the critical aggregation concentration (CAC), usually a few orders of magnitude lower than the critical micelle concentration (CMC) of the free surfactant. Unlike the situation for nonionic polymer/ionic surfactant systems wherein complexation causes charge accumulation, the polyelectrolyte complex usually cannot coexist with free micelles because precipitation is observed as the addition of ionic surfactant brings the polyelectrolyte close to charge neutralization.[7–17]

Dublin and co-workers[18–27] have demonstrated that the strong electrostatic interaction between polyelectrolytes

* To whom correspondence should be addressed.

® Abstract published in *Advance ACS Abstracts,* June 15, 1995.

(1) Robb, I. D. In *Anionc Surfactants, Physical Chemistry of Surfactant Action*; Lucassen-Reynders, E. H. Ed.; Marcel Dekker: New York, 1981; p. 109.
(2) Goddard, E. D. *Colloids Surf.* **1986**, *19*, 301.
(3) Hayakawa, K.; Kwak, J. C. T. In *Cationic Surfactants. Physical Chemistry*; Rubingh, D. N.; Holland, P. M., Eds.; Marcel Dekker: New York, 1991; Chapter 5, p 189.
(4) Piculell, B.; Lindman, B. *Adv. Colloid Interface Sci.* **1992**, *41*, 149.
(5) Lindman, B.; Thalberg, K. In *Interactions of Surfactants with Polymers and Proteins*; Goddard, E. D., Ananthapadmanabhan, K. P., Eds.; CRC Press: Boca Raton, FL, 1993; Chapter 5.
(6) Li, Y.; Dubin, P. L. In *Structure and Flow in Surfactant Solutions*; Herb, C. A., Prud'homme, R. K., Eds.; ACS Symposium Series 578; American Chemical Society: Washington, DC, 1994; Chapter 23, p. 320.
(7) Goddard, E. D.; Hannan, R. B. *J. Colloid Interface Sci.* **1976**, *55*, 73.
(8) Ohbu, K.; Hiraishi, O., Kashiwa, I. *J. Am. Oil Chem. Soc.* **1982**, *59*, 108.
(9) Goddard, E. D.; Phillips, T. S.; Hannan, R. B. *J. Soc. Cosmet. Chem.* **1975**, *26*, 461.
(10) Goddard, E. D.; Hannan, R. B. *J. Colloid Interface Sci.* **1976**, *55*, 73.
(11) Goddard, E. D.; Hannan, R. B. *J. Am. Oil Chem. Soc.* **1977**, *54*, 561.
(12) Thalberg, K.; Lindman, B. *J. Phys. Chem.* **1989**, *93*, 1478.
(13) Thalberg, K.; Lindman, B.; Karlström, G. *J. Phys. Chem.* **1990**, *94*, 4289.
(14) Thalberg, K.; Lindman, B.; Karlström, G. *J. Phys. Chem.* **1991**, *95*, 6004.
(15) Thalberg, K.; Lindman, B.; Karlström, G. *J. Phys. Chem.* **1991**, *95*, 3370.
(16) Thalberg, K.; Lindman, B.; Bergfeldt, K. *Langmuir* **1991**, *7*, 2893.
(17) Hansson, P.; Almgren, M. *Langmuir* **1994**, *10*, 2893.
(18) Dubin, P. L.; Oteri, R. *J. Colloid Interface Sci.* **1983**, *95*, 453.
(19) Dubin, P. L.; Davis, D. D. *Macromolecules* **1984**, *17*, 1294.
(20) Dubin, P. L.; Davis, D. D. *Colloids Surf.* **1985**, *13*, 113.
(21) Dubin, P. L.; Rigsbee, D. R.; McQuigg, D. W. *J. Colloid Interface Sci.* **1985**, *105*, 509.
(22) Dubin, P. L.; Rigsbee, D. R.; Gan, L.-M.; Fallon, M. A. *Macromolecules* **1988**, *21*, 2555.
(23) Dubin, P. L.; Thé, S. S.; McQuigg, D. W.; Chew, C. H.; Gan, L.-M. *Langmuir* **1989**, *5*, 89.
(24) Dubin, P. L.; Vea, M. E.; Fallon, M. A.; Thé, S. S.; Rigsbee, D. R.; Gan, L.-M. *Langmuir* **1990**, *6*, 1422.
(25) Dubin, P. L.; Thé, S. S.; McQuigg, D. W.; Gan, L.-M.; Chew, C. H.; *Macromolecules* **1990**, *23*, 2500.

0743-7463/95/2411-2486$09.00/0

and micelles of opposite charge may be attenuated by using mixed micelles of nonionic and ionic surfactants. Thus Dubin and Oteri[18] showed that the interaction between poly(dimethyldiallylammonium chloride) (PDMDAAC) and mixed micelles of sodium dodecylsulfate (SDS) and Triton X-100 (TX100) takes place only when a critical mole ratio Y_c of SDS to TX100 has been reached, where Y, defined as [SDS]/([SDS] + [TX100]), is proportional to the mixed micelle average surface charge density. In addition to the microscopic phase transition at Y_c corresponding to the reversible formation of soluble polyelectrolyte-mixed micelle complexes, Dubin and Oteri[18] observed a second transition, corresponding to bulk phase separation, at a higher Y value, denoted by Y_p. Y_p usually exceeds Y_c by about 50% to 100%. The region between Y_c and Y_p represents a range of micelle surface charge density wherein soluble, reversible complexes can form. At moderate to high polyelectrolyte concentration, a maximum in the turbidity versus Y curve is observed between Y_c and Y_p. A number of techniques have been used to study the soluble complex formation.[18-27] In particular, a recent study,[28] showed that the scattered intensity and the apparent hydrodynamic radius (R_h) of complexes reached a maximum at $W = 0.09$, where W is defined as the weight ratio of PDMDAAC to TX100-SDS. The electrophoretic mobility changes from negative to positive and is close to zero at this same stoichiometry, which corresponds to a 1:1 bulk charge ratio of PDMDAAC to TX100-SDS. However, *no* precipitation or coacervation (liquid–liquid phase separation into a dense coacervate phase relatively concentrated in the solutes and a dilute equilibrium phase) is observed even when the electrophoretic mobility is close to zero, in direct contrast to literature reports on polyelectrolyte/surfactant systems.[7] A partially interacted model was proposed[28] for the PDMDAAC/TX100-SDS complexes wherein only part of the positive charge in PDMDAAC and part of the negative charge in TX100-SDS compensate each other.

While electrostatically driven complex coacervation (according to Piculell and Lindman[4] a more descriptive term for complex coacervation is "associative phase separation") between polyelectrolytes has been known for many years,[29] similar phenomena involving polyelectrolytes and colloidal particles have received less attention. Such coacervates are of interest in several areas. For example, the coacervation of proteins with polyelectrolytes reveals possible methods for large-scale protein separation[30] or for enzyme immobilization.[31] In polyelectrolyte/micelle systems, the formation of a dense phase of entrapped micelles affords intriguing possibilities for solubilization. Therefore the relationship between the structure of soluble complexes and the formation of coacervates merits elucidation. This paper focuses on the phase boundary of the PDMDAAC/TX100-SDS system and the structure of soluble complexes, particularly at conditions very close to the phase boundary. The information obtained can also be compared with theories developed for polycation/polyanion mixtures.[32-46]

Experimental Section

Materials and Solution Preparation. The PDMDAAC sample used in this study was synthesized by free radical polymerization in aqueous solution to a conversion of 12% using a cationic azo initiator. Purification and isolation of the polymer were carried out by ultrafiltration using a 30 K nominal MW cut-off membrane, followed by freeze-drying. The purified sample has a weight-average molecular weight (M_w) of 256K (from light scattering) and a number-average molecular weight (M_n) of 170K (from osmometry). TX100 was purchased from Aldrich, and SDS, from Fluka. Ionic strength was adjusted with NaCl from Fisher. TX100, SDS, and NaCl were used without further purification. Milli-Q water was used throughout this work. Solutions were prepared by slowly (under stirring) adding 60 mM SDS in 0.4 M NaCl to a solution of 40 mM TX100 and known concentration of PDMDAAC (C_p), also in 0.4 M NaCl, up to $Y = 0.3$, which corresponds to soluble complex formation. The solutions were stirred for at least 2 h prior to any measurements. Since the CMC for TX100-SDS under such conditions is less than 0.2 mM, these solutions are polyelectrolyte/micelle systems.

Turbidimetry. Turbidity measurements, reported as $100 - \%T$, were performed at 420 nm using a Brinkman PC800 probe colorimeter equipped with a 2-cm path length fiber optics probe at 24 ± 1 °C.

Dynamic Light Scattering. The diluted solutions were passed through 0.45-μm filters (Life Science Products). Most of the dynamic light scattering measurements were carried out at 24 ± 1 °C and at angles from 45 to 120 ° using a Brookhaven Instruments system equipped with a 72-channel digital correlator (BI-2030AT) and an Omnichrome air-cooled 200 mW argon-ion laser operating at a wavelength in vacuum $\lambda_0 = 488$ nm.

In the self-beating mode of dynamic light scattering, the measured photoelectron count autocorrelation function $G^{(2)}(\tau,q)$ for a detector with a finite effector photocathode area has the form[47-49]

$$G^{(2)}(\tau,q) = N_s\langle n\rangle^2(1 + b|g^{(1)}(\tau,q)|^2) \quad (1)$$

where $g^{(1)}(\tau,q)$ is the first-order scattered electric field (E_s) time correlation function; τ, the delay time; $\langle n\rangle$, the mean counts per sample; N_s, the total number of samples; A ($=N_s\langle n\rangle^2$), the baseline; b, a spatial coherence factor depending upon the experimental set-up and taken as an unknown parameter in the data fitting procedure; and $q = (4\pi n/\lambda_0)\sin(\Theta/2)$ with n and Θ being the refractive index of the scattering medium and the scattering angle, respectively.

For a solution of polydisperse particles, $g^{(1)}(\tau,q)$ has the form

$$|g^{(1)}(\tau,q)| = \int_0^\infty G(\Gamma,q)e^{-(\Gamma(q)\tau}\,d\Gamma \quad (2)$$

where $G(\Gamma,q)$ is the normalized distribution of line width Γ measured at a fixed value of q. In the present study, a CONTIN algorithm was used to obtain the average Γ and its distribution of the complex mode and the free micelle mode.[50] The apparent translational diffusion coefficient, D, is related to Γ by $D = \Gamma/q^2$. R_h can then be estimated via the Stokes–Einstein equation

(26) Xia, J.; Zhang, H.; Rigsbee, D. R.; Dubin, P. L.; Shaikh, T. *Macromolecules* **1993**, *26*, 2759.
(27) Li, Y.; Xia, J.; Dubin, P. L. *Macromolecules* **1994**, *27*, 7049.
(28) Li, Y.; Dubin, P. L.; Havel, H. A.; Edwards, S. L.; Dautzenberg, H. *Macromolecules*, accepted.
(29) Bungenberg de Jong, M. G. In *Colloid Science*; Kruyt, G. R., Ed.; Elsevier: New York, 1990; Vol II, Chapter X, pp 335–432.
(30) Dubin, P. L.; Gao, J.; Mattison, K. *Sep. Purif. Methods* **1994**, *23*, 1.
(31) Dubin, P. L.; Muhoberac, B.; Xia, J. Pat. Pending.
(32) Voorn, M. J. *Recl. Trav. Chim.* **1956**, *75*, 317.
(33) Voorn, M. J. *Recl. Trav. Chim.* **1956**, *75*, 405.
(34) Voorn, M. J. *Recl. Trav. Chim.* **1956**, *75*, 427.
(35) Voorn, M. J. *Recl. Trav. Chim.* **1956**, *75*, 925.
(36) Voorn, M. J. *Recl. Trav. Chim.* **1956**, *75*, 1021.
(37) Overbeek, J. Th. G.; Voorn, M. J. *J. Cell. Comp. Physiol.* **1957**, *49* (*Suppl. 1*), 7.
(38) Voorn, M. J. *Fortschr. Hochpolym.-Forsch.* **1959**, *1*, 192.
(39) Veis, A.; Aranyi, C. *J. Phys. Chem.* **1960**, *64*, 1203.
(40) Veis, A. *J. Phys. Chem.* **1961**, *65*, 1798.
(41) Veis, A. *J. Phys. Chem.* **1963**, *67*, 1960.
(42) Veis, A.; Bodor, E.; Mussell, S. *Biopolymers* **1967**, *5*, 37.
(43) Nakajima, A.; Sato, H. *Biopolymers* **1972**, *10*, 1345.
(44) Sato, H.; Nakajima, A. *Colloid Polym. Sci.* **1974**, *252*, 944.
(45) Tainaka, K. *J. Phys. Soc. Jpn.* **1979**, *46*, 1899.
(46) Tainaka, K. *Biopolymers* **1980**, *19*, 1289.
(47) Chu, B. *Laser Light Scattering*; Academic Press: New York, 1991.
(48) Berne, B. J.; Pecora, R. *Dynamic Light Scattering*; Wiley: New York, 1976.
(49) Schmitz, K. S. *An Introduction to Dynamic Light Scattering by Macromolecules*; Academic Press: Boston, MA, 1990.
(50) Provencher, S. W. *J. Chem. Phys.* **1976**, *64*, 2772; *Makromol. Chem.* **1979**, *180*, 201.

$$D_0 = k_B T/(6\pi\eta R_h) \quad (3)$$

where k_B is the Boltzmann constant; T is the absolute temperature; and η is the solvent viscosity.

Static Light Scattering. The excess Rayleigh ratio $R(q)$ of the complex at finite q and finite complex concentration C_x has the form[47]

$$HC_x/R(q) = (1/M_{w,x})(1 + R_g^2 q^2/3) + 2A_2 C_x \quad (4)$$

where $M_{w,x}$ is the weight-averaged molar mass of the complex; A_2 is the second virial coefficient; and $H = 4\pi^2 n^2 (dn/dc)^2/(N_A \lambda_0)$ with dn/dc and N_A being the refractive index increment and Avogadro's number, respectively.

The low concentration of PDMDAAC in this study justifies the following approximation:

$$HC_x/R(q) \approx (1/M_{w,x})(1 + R_g^2 q^2/3) \quad (5)$$

In the limit of $q \to 0$, eq 5 can be written as

$$I(q \to 0) \approx H' C_x M_{w,x} (dn/dc)^2 \quad (6)$$

where H' is a constant. It is further assumed that $C_x = (1+\beta)C_p$ where β is the degree of binding, i.e., the mass of surfactant bound per unit mass polyelectrolyte. Equation 6 can then be written as

$$I(q \to 0) \approx H'(1+\beta)^2 C_p \alpha M_{w,p} (dn/dc)^2 \quad (7)$$

where α and $M_{w,p}$ are the number of the polymer in one complex and the weight-average molecular weight of the polymer, respectively. Therefore, in a plot of $I(q \to 0)$ *vs* C_p, a change in slope implies a change in β or dn/dc. For example, if interpolymer complexes start to form with increasing C_p, an increased slope should be observed.

Most static light scattering measurements were performed at 24 ± 1 °C and at angles from 25 to 145 ° along with dynamic light scattering measurements on the same solutions as described above.

Electrophoretic Light Scattering. Electrophoretic light scattering was carried out at 25 °C at four angles (8.6, 17.1, 25.6, 34.2°) using a DELSA 440 apparatus from Coulter Instrument Co. The electric field was applied at a constant current of 8−14 mA. The electrophoretic cell has a rectangular cross section connecting the hemispherical cavities in each electrode. The total sample volume was about 1 mL. The measured electrophoretic mobility, U, was the average value at the stationary layer and at the four angles. More details about electrophoretic light scattering can be found in ref 51.

Results and Discussion

Phase Boundary. At high total concentration of TX100-SDS and PDMDAAC (e.g., [TX100] = 30 mM), Y = 0.3, and 0.4 M NaCl, the PDMDAAC/TX100-SDS system forms soluble complexes, regardless of W.[28] The phase boundary of PDMDAAC/TX100-SDS system was established by diluting such systems with 0.4 M NaCl (at constant ionic strength and W) until a sharp increase in turbidity was observed. The TX100 concentration corresponding to the onset of coacervation was denoted as $C_{TX\text{-}100,c}$. The results from such dilution are presented by the open circles in Figure 1a. In order to insure that this is a true phase boundary rather than a kinetically controlled phenomenon, the phase boundary was checked by increasing the polymer concentration from solutions with $W = 0.01$, with the results presented in Figure 1a as triangles. The good agreement of the two sets of results verifies that this is an equilibrium phase boundary.

(51) Ware, B.; Haas, D. D. In *Fast Methods in Physical Biochemistry and Cell Biology*; Sha'afi, R. I., Fernandez, S. M., Eds.; Elsevier: Amsterdam, 1983; Chapter 8.

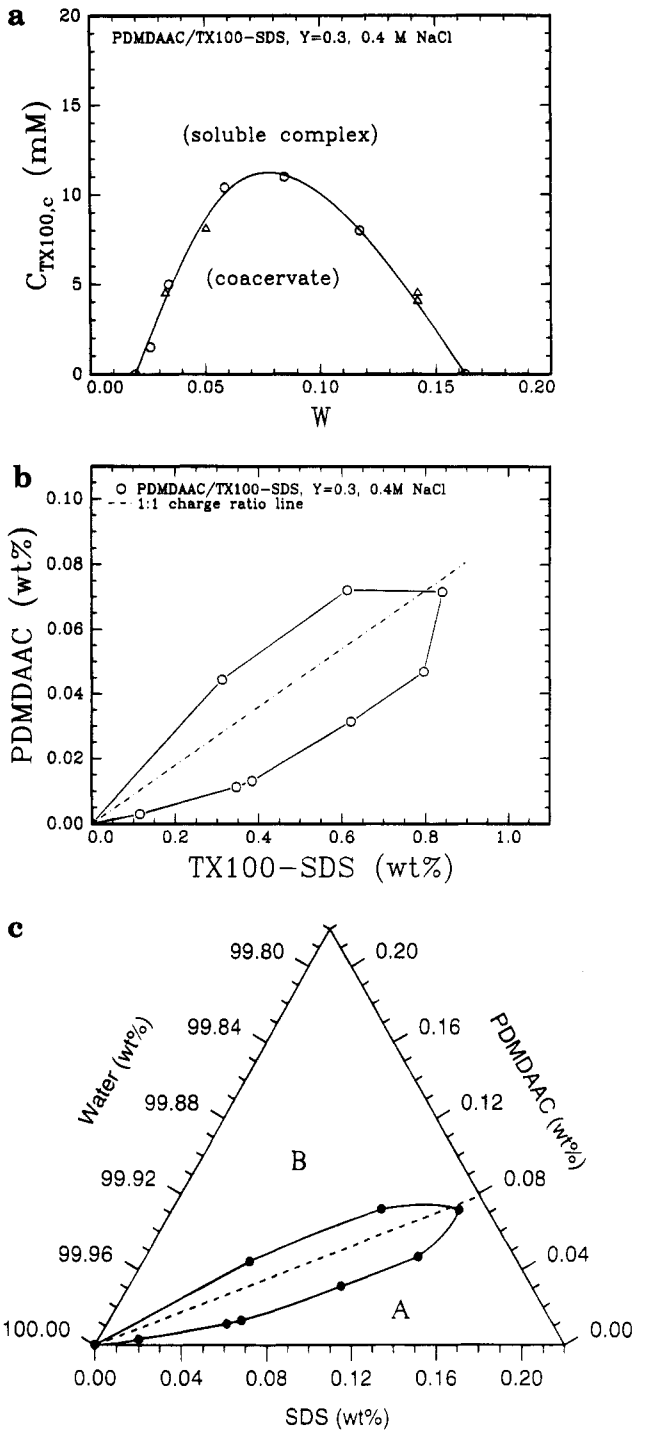

Figure 1. (a) Phase boundary of soluble complexes vs. coacervate for PDMDAAC/TX100-SDS system. The open circles are results from dilution with 0.4 M NaCl, and the triangles from increasing polymer concentration. (b and c) Simplified presentations of the phase boundary for PDMDAAC/TX100-SDS system in 0.4 M NaCl with Y = 0.3. The enclosed area in Figure 1c represents coacervation; the bright area, soluble complex formation. The amount of TX100 can be obtained from Y = 0.3. The lines are for guiding the eyes only.

In order to facilitate a comparison between this phase boundary and literature reports for the gelatin/gum arabic/water system,[29] the results in Figure 1a were presented in the phase diagram form of Figure 1b. Although we could determine the point of coacervation, the composition of the two phases could not be analyzed because the volume of the coacervate is too small. Since parts a and b of Figure 1 only tell us at what condition coacervation takes place, but not the composition of the two phases at

coacervation, they are strictly speaking phase boundaries, not phase diagrams. The phase boundary shape in Figure 1b is very similar to that reported by Bungenberg de Jong for the gelatin/gum arabic/water system. On the other hand, the disappearance of coacervate with decreasing total concentration is not observed here, and the coacervation region is much smaller than in the gelatin/gum arabic/water system.

The phase boundary of PDMDAAC/TX100-SDS system can also be presented in Figure 1c in the manner reported by Thalberg *et al.*[12-16] and by Hansson and Almgren[17] for oppositely charged surfactant/polyelectrolyte systems; this does not show the concentration of TX100 and NaCl although the former can be calculated for $Y = 0.3$. The shape of our phase boundary resembles those presented in refs 12–17 but the coacervation region is about 2 orders of magnitude smaller. In a solution of PDMDAAC and SDS (corresponding to $Y = 1.0$), precipitation takes place over a wide range of SDS concentration when the charge ratio of PDMDAAC to SDS is close to 1:1.[16,18] The fact that a reduction of Y from 1.0 to 0.3 can introduce such a significant effect on the size of the phase separation shows that the micelle charge density plays a dominant role in phase behavior. In principle, phase separation region could take place in some undetermined regime with micelles of low charge density, i.e., a non-complex-forming system. But in the strongly interacting system we have chosen to study here, complexation always occurs.

In the polyelectrolyte/polyelectrolyte systems the chain length and charge density of the polycation are often similar to those for the polyanion so that the two form a "stoichiometric" complex.[32-46] In contrast, the polyelectrolyte and micelle here differ with respect to geometry, charge spacing, and flexibility. Each free TX100-SDS mixed micelle contains about 110 sulfate groups,[26] and each PDMDAAC molecule contains 1600 quaternary ammonium groups. The distance between two adjacent quaternary ammonium groups in PDMDAAC is about 0.7 nm, and that for the two adjacent sulfate groups in the micelle is about 3 nm.[52] Even allowing for the possibility of SDS migration within the micelle upon complex formation, the polyion/micelle system is very asymmetric. This and the difference in shape of the micelles and polyelectrolytes are fundamental differences between polyelectrolyte-micelle systems and polyelectrolyte-polyelectrolyte systems. Despite the lack of structural or electrostatic complementarity, the coacervation region in Figure 1a–c is almost symmetrical around the 1:1 bulk charge ratio. Such a phenomenon cannot be explained by complementary ion-pairing. The apparent "stoichiometric" relation for the polyelectrolyte/micelle system is achieved through binding of some particular (large) number of micelles to one PDMDAAC molecule.[18-28]

Effect of Dilution on Structure in the Soluble Complex Region. Figure 2 shows a typical CONTIN distribution for PDMDAAC/TX100-SDS at low W. In 0.4 M NaCl, the free TX100-SDS and PDMDAAC have R_h values of 8–9 and 15 nm, respectively,[26-28] which allows us to identify the two modes as free micelle and complex, respectively. Results presented in Figure 2 as well as in Figure 4a–c are from the excess-micelle side of the soluble complex region, i.e., from region A in Figure 1c. In this region ($W < 0.09$) the soluble complexes have negative charge, as shown in Figure 3. Figure 4a shows the effect of dilution on the scattered intensity corrected for the

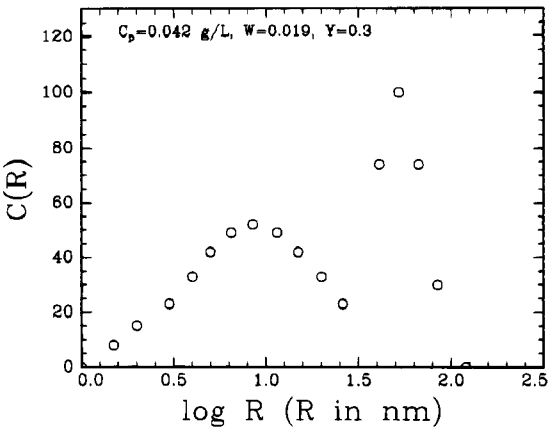

Figure 2. CONTIN distribution of the PDMDAAC/TX100-SDS complexes coexisting with free micelles. PDMDAAC concentration is 0.042 g/L; $W = 0.019$; $Y = 0.3$. $C(R)$ is the scattering intensity averaged distribution of effective radius R.

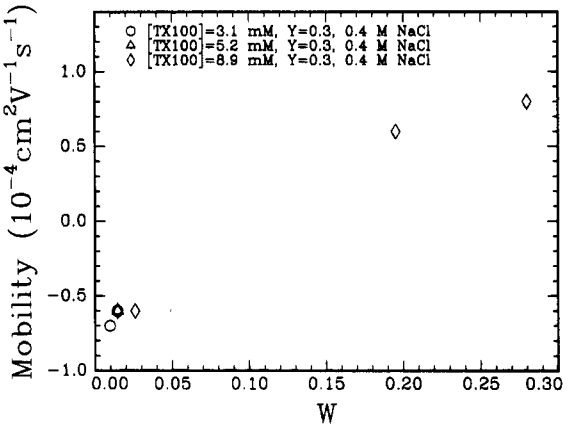

Figure 3. Electrophoretic mobility of the PDMDAAC/TX100-SDS complexes as a function of W at $Y = 0.3$ and different surfactant concentration. Between $W = 0.05$ and 0.15 the particles are too big for electrophoretic light scattering.

scattering background of 0.4 M NaCl/water. If no structure change were involved, the scattered intensity would decrease linearly down to zero upon dilution (eq 6). The slight upward curvature in Figure 4a implies a dissociation of the complexes upon dilution. This is in agreement with the dynamic light scattering data presented in Figure 4b, in which the decrease in R_h is too great to be attributed solely to a concentration effect. There are two possible mechanisms for this dissociation: transition of interpolymer complexes into intrapolymer complexes, or the release of bound micelles. However, in the latter case, the electrophoretic mobility of the complexes should become more positive, which is contradicted by the results shown in Figure 4c. It is thus more likely that dilution leads to dissociation of interpolymer complexes into intra-polymer complexes.

The electrophoretic mobility of an intra-polymer complex, $U_{x,0}$, is related to the total charge of the complexes, $q_{x,0}$, and the friction coefficient $f_{x,0}$ by

$$U_{x,0} = q_{x,0}/f_{x,0} = (q_p\alpha - n_m q_m \beta)/f_{x,0} \quad (8)$$

where n_m, q_p, q_m, α, and β are, respectively, the number of micelles per complex, the charge of PDMDAAC, the charge of micelles, a constant to take into account the counterions accompanying PDMDAAC, and a constant to take into account the counterions accompanying the

(52) The value of 3 nm represents the average distance between adjacent sulfate groups in the micelle. We cannot exclude the possibility of lateral migration upon binding to the PDMDAAC chain to accommodate the small distance between adjacent quaternary ammonium groups.

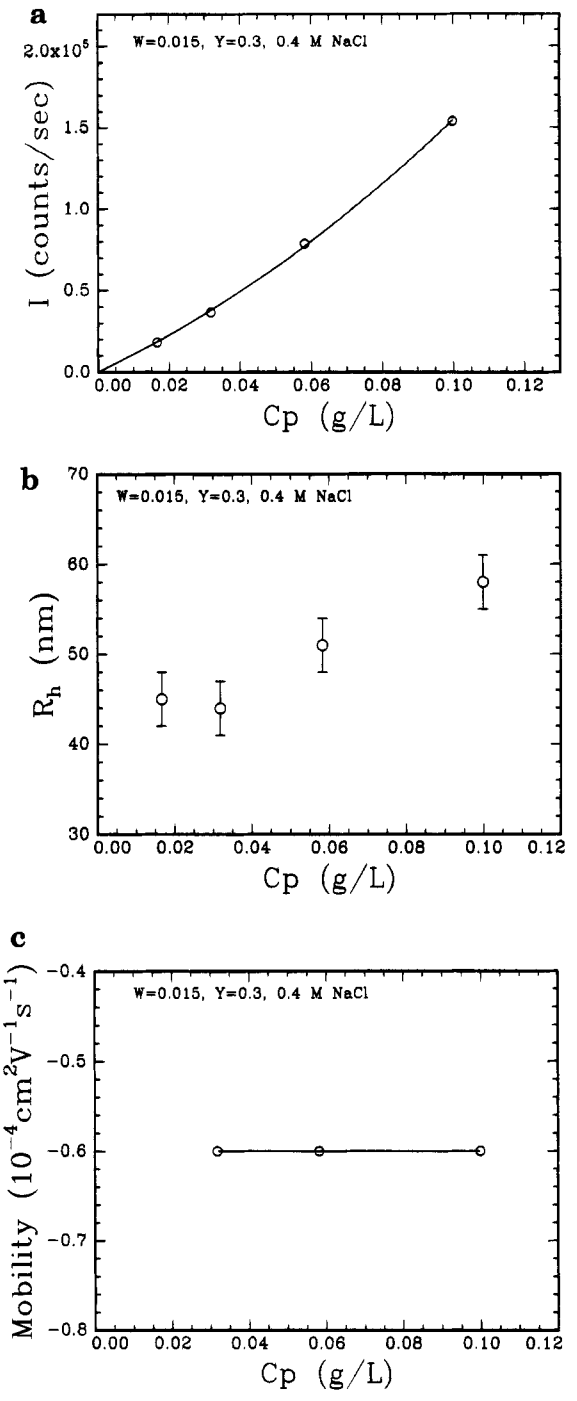

Figure 4. Scattered intensity (a), hydrodynamic radius R_h (b), and electrophoretic mobility (c) of the PDMDAAC/TX100-SDS complexes as a function of PDMDAAC concentration, C_p, at $W = 0.015$, and $Y = 0.3$. The lines are for guiding the eyes only. R_h has an uncertainty of about 10%.

micelles. When n intrapolymer complexes form an interpolymer complex, let us assume that the local hydrodynamic properties remains unchanged. Therefore the friction coefficient of the inter-polymer complex is $f_{x,n} = nf_{x,0}$ and the charge is $(nq_p\alpha = nm_mq_m\beta)$, so that the mobility is unchanged. Put differently, inter- and intrapolymer complexes behave electrophoretically as polyelectrolytes of different molecular weights and with equivalent overall charge density. At high ionic strength, polyelectrolytes show free-draining behavior in electrophoresis and the electrophoretic mobility is independent of molecular weight.[53]

Figure 5 shows a typical CONTIN distribution of PDMDAAC/TX100-SDS at relatively high W ($W = 0.279$).

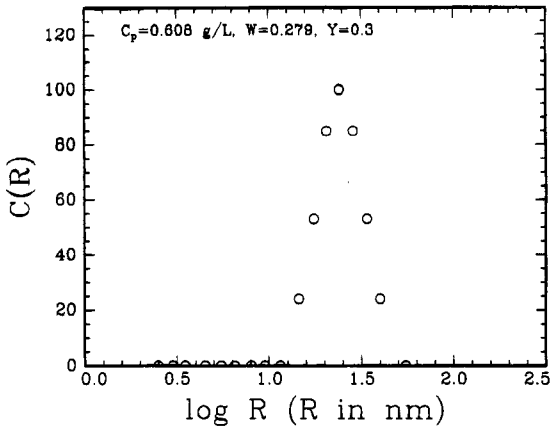

Figure 5. CONTIN distribution of the PDMDAAC/TX100-SDS complexes without free micelles. PDMDAAC concentration is 0.608 g/L; $W = 0.279$; $Y = 0.3$. $C(R)$ is the scattering intensity averaged distribution of effective radius R.

These conditions correspond to the part of the soluble complex region in which the bulk concentration of cationic quaternary ammonium group in PDMDAAC is in excess relative to the concentration of anionic sulfate groups in SDS, i.e., to region B in Figure 1c. No free micelles were observed, and the system forms fairly monodisperse complexes. The complexes in this region are positively charged, as shown in Figure 3. Parts a and b of Figure 6 show the dilution effect at $W = 0.279$ on the scattered intensity (corrected for the scattering background of 0.4 M NaCl/water) and on R_h of the complexes, respectively. The effect of dilution may again be explained as disassociation of interpolymer complexes into intrapolymer complexes.

The results from Figures 2–6 shown above establish the formation of soluble complexes under a wide range of conditions. They are consistent with the hypothesis that dilution can change interpolymer complexes into intrapolymer complexes, while the local structure of complexes, as indicated by the electrophoretic mobility, does not change significantly. Thus, the effects we see are not simply transitions from semidilute to dilute regimes, but rather correspond to changes in complex structure at the supermolecular level.

Effect of W on Complex Structure. Figure 7a shows the effect of W, in the excess surfactant region, on R_h of the complex. With increasing W, R_h changes very little until $W \cong 0.02$, at which point it increases sharply. Figure 7b shows the estimated excess scattered intensity (extrapolated to $q = 0$) of the complex. The estimated excess scattered intensity from complexes were obtained by subtracting from the measured value the scattered intensity of polymer-free micelles at the same concentration. This approach disregards the diminution in free micelle concentration for the complex system, but may be a reasonable approximation due to the excess of free micelles and their low scattering intensity. I, like R_h, shows an abrupt increase at $W \cong 0.02$. The results in Figure 7a,b may be explained as follows. Below $W \cong 0.02$, only intrapolymer complexes are formed. Their number increases with W, with no change in size and molar mass. Above $W \cong 0.02$, interpolymer complexes start to form, resulting in a large increase in both R_h and the scattered intensity. Further increase in W drives the system into coacervation. Thus the interpolymer complex seems to be a precursor of coacervation. Unfortunately, charac-

(53) Armstrong, R. W.; Strauss, U. P. *Encycl. Polym. Sci. Technol.* **1969**, *10*, 781.

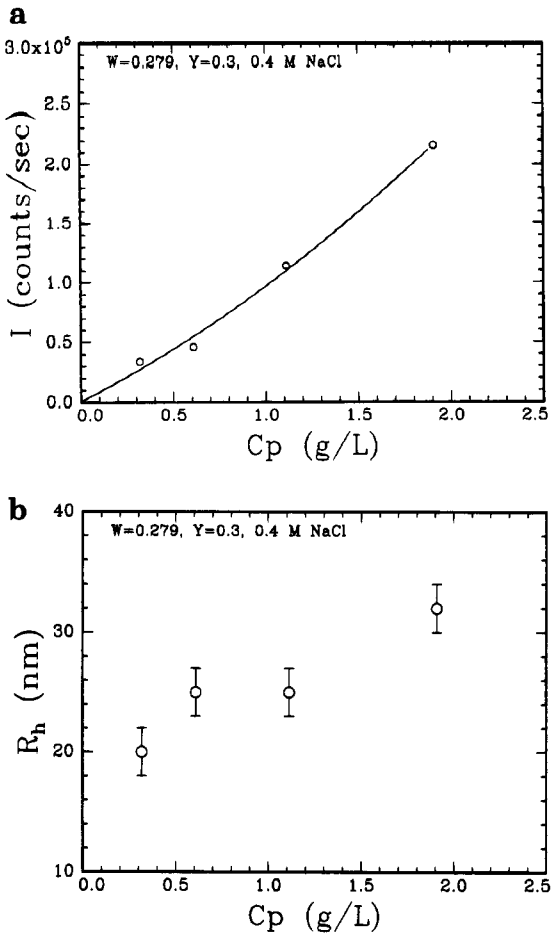

Figure 6. Scattered density (a) and hydrodynamic radius R_h (b) of the PDMDAAC/TX100-SDS complexes as a function of PDMDAAC concentration, C_p at $W = 0.279$ and $Y = 0.3$. The line is for guiding the eyes only. R_h has an uncertainty of about 10%.

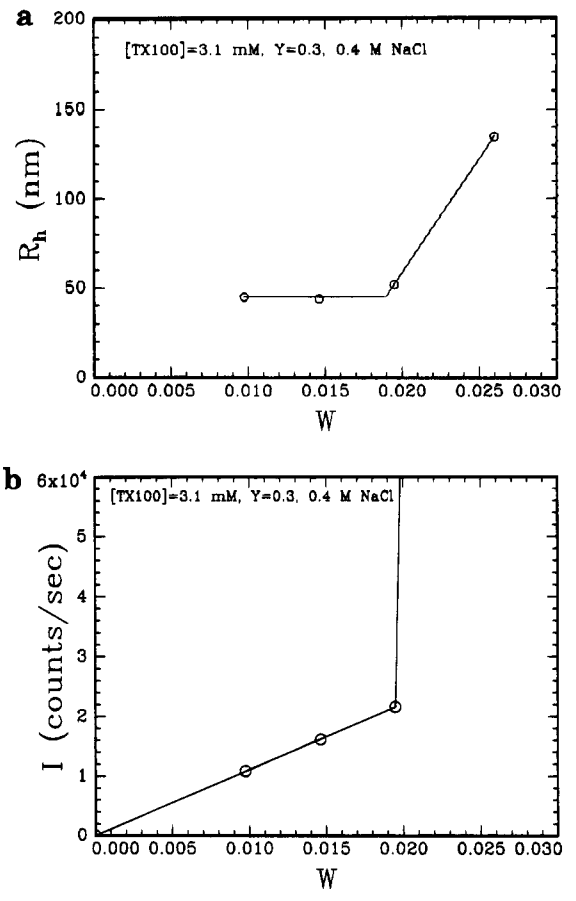

Figure 7. Hydrodynamic radius (a) and scattered intensity (b) of PDMDAAC/TX100-SDS complexes as a function of W at $Y = 0.3$ and 3.1 mM TX100. The lines are for guiding the eyes only.

terization of the interpolymer ⇌ coacervate transition by light scattering is prevented by the large size of the coacervate.

Comparison with Complex Coacervation Theories. Although there has been no theoretical work on the complex coacervation of polyelectrolytes and oppositely charged mixed micelles, several theoretical models are available for polyelectrolyte mixtures[32-46] and their applicability has been discussed by Burgess.[54] The first is the Voorn-Overbeek theory,[32-38] developed on the basis of the experimental data by Bungenberg de Jong.[29] The theory has several assumptions: (1) there is a random chain distribution of macromolecules in both phases; (2) solvent−solute interactions are negligible; and (3) charges are distributed throughout the solution without regard to the fact that they reside on the polymer chains. Site-specific interactions lead to precipitation instead of coacervation. According to Voorn and Overbeek, the primary factors which affect coacervation are the charge densities and the molecular weight of the polyelectrolytes. In order for coacervation to take place, the charge densities and molecular weights have to be high. The formation of a concentrated coacervate phase is driven by a gain in electrostatic free energy at the expense of a decrease in total entropy.[42] This model was later refined by Nakajima and Sato[43,44] who included the Flory−Huggins interaction parameter and altered the electrostatic term. However, Veis[39-42] showed that the coacervation behavior in a gelatin/gelatin system does not agree with the critical conditions predicted by the Voorn−Overbeek theory. In order to interpret these observations, Veis developed a so-called dilute phase aggregate model, in which coacervation is considered as a two-step process. First, the oppositely charged polyelectrolytes aggregate upon mixing due to electrostatic interaction. Some of these aggregates rearrange to form coacervate, while some are retained in the dilute phase. According to Veis's model, coacervation is driven by the gain in configurational entropy from rearranging the aggregates into a randomly distributed coacervation phase. More recently, Tainaka[45,46] assumed the aggregates to be in both dilute and coacervate phases.

A major difference among the aforementioned models is that Veis's and Tainaka's models assumed formation of aggregates (corresponding to complex in the present work). The formation of soluble PDMDAAC/TX100-SDS complexes under a wide range of conditions supports these models. The models by Voorn and Overbeek and by Nakajima and Sato cannot be applied to this system. However, the formation of interpolymer complexes in PDMDAAC/TX100-SDS systems is not considered by Veis and Tainaka.

Tainaka's model can qualitatively explain the effect of charge density and chain length of the components on coacervation. According to Tainaka, both the charge density and the chain length of polyelectrolytes must fall within a certain range for coacervation to occur. If the charge density or chain length are too high, precipitation will take place because of strong long-range attractive forces among aggregates. If the charge density or the chain length are too low, the dilute solution is stabilized by short-range repulsive forces and coacervation will not take place. Experimentally, Dubin and Oteri[18] showed

(54) Burgess, D. J. *J. Colloid Interface Sci.* **1990**, *140*, 227.

precipitation instead of coacervation when SDS ($Y = 1$) was added to PDMDAAC solution, and the present authors[27] showed that PDMDAAC/TX100-SDS system does not coacervate when the chain length of PDMDAAC is reduced from 590K to 50K.[27]

Coacervation does not occur at high total concentration of PDMDAAC and TX100-SDS even for mixtures near the 1:1 bulk charge ratio. This phenomenon has been observed in polyelectrolyte/polyelectrolyte,[29,42,43,45,55] polyelectrolyte/protein,[56] and polyelectrolyte/surfactant[12-17] systems, and is termed "self-suppression".[32-46,54] Both Veis and Tainaka attempted to explain such phase behavior for polyelectrolyte/polyelectrolyte system. According to Veis, polyelectrolyte domains overlap with increasing total concentration, and the entropy gain due to coacervation diminishes. However, the coacervation region in Figure 1c is much smaller than those for either polyelectrolyte/polyelectrolyte or polyelectrolyte/surfactant systems,[12-17] corresponding to a very low concentration. For example, at $W = 0.09$, a self-suppression starts around [PDMDAAC] = 0.8 g/L, well below the overlap concentration of $C^* \cong 10$ g/L. According to Tainaka, when the total concentration is high the size of the aggregates is decreased. Both the second and the third virial coefficients are large, and the aggregates are stabilized. This point is hard to assess here. For polyelectrolyte/surfactant systems, Thalberg *et al.*[12-16] calculated the phase diagrams using the Flory–Huggins theory and treating the surfactant as a second polymer with adjustable polymerization numbers. Assuming that the treatment of Thalberg *et al.* works in the PDMDAAC/TX100-SDS system, the small coacervation region of the PDMDAAC/TX100-SDS system could be explained as due to weak interactions and consequently a less negative Flory-Huggins interaction parameter between PDMDAAC and TX100-SDS compared to PDMDAAC and SDS. However, more quantitative explanation probably is not very meaningful because the treatment by Thalberg *et al.* involves five adjustable parameters.

(55) Lenk, T.; Thies, C. in *Coulombic Interactions in Macromolecular Systems*; Eisenberg, A., Bailey, F. E., Eds.; ACS Symposium Series 302; American Chemical Society: Washington, DC, 1986.

(56) Singh, O. N.; Burgess, D. J. *J. Pharm. Pharmacol.* **1989**, *41*, 670.

Concluding Remarks

This paper has explored the relationship between soluble complex formation and coacervation in PDMDAAC/TX100-SDS with $Y = 0.3$ and in 0.4 M NaCl. Coacervation takes place when the total concentration of both micelles and PDMDAAC is very low and the weight ratio of PDMDAAC to TX100-SDS, W, is close to 0.09, corresponding to a 1:1 bulk charge ratio of PDMDAAC to TX100-SDS. Although the shape of the coacervation region is similar to those of polyelectrolyte/surfactant systems without nonionic surfactant, the coacervation region of the present PDMDAAC/TX100-SDS system is over 2 orders of magnitude smaller. This is explained on the basis of the attenuation of interactions resulting from the incorporation of TX100 into the micelles. In the soluble complex region, dilution with 0.4 M NaCl dissociates interpolymer complexes into intrapolymer complexes, while the electrophoretic mobility of the complexes remains unchanged, implying free-draining polyelectrolyte behavior. Increase in W first causes an increase in the number of intrapolymer complexes, following by formation of inter-polymer complexes and coacervation. Further increase in W redissolves the coacervate.

The formation of soluble complexes under a wide range of conditions supports the theoretical models of complex coacervation by Veis and by Tainaka. The models can also explain the effect of charge density and chain length on coacervation. However, none of the theories predict interpolymer complex formation. A quantitative explanation of why the coacervation region in PDMDAAC/TX100-SDS is so small and why self-suppression occurs at such a low total concentration of TX100-SDS and PDMDAAC is still lacking.

Acknowledgment. The support of Grant DMR-9311433 from the National Science Foundation, jointly funded by the Division of Materials Research and Chemical Transport Systems, is gratefully acknowledged. We thank Professor Arthur Veis for his helpful comments.

LA950016G